Check for updates

BiVO$_4$-polyvinyl alcohol composites: a novel approach to wastewater treatment with antimicrobial efficacy

Rabia Shahzad,†[a] Sabah Kausar, [iD] †[a] Tahir Iqbal,†*[a] Sumera Afsheen,[b] Aqsa Ashraf,[a] Abdallah M. Elgorban,[c] Hind A. AL-Shwaiman,[c] Zain Ashfaq,[d] Atif Mossad Ali[e] and M. A. Sayed[e]

Pure BiVO$_4$, PVA, and BiVO$_4$/PVA (1 : 3) nanocomposite were synthesized using a straight forward coprecipitation technique to improve the photocatalytic degradation of reactive yellow dye. The optical and morphological properties of synthesized nanostructures were characterized by XRD, SEM, EDX, FTIR, PL, and UV-via spectra. The optical properties of pure BiVO$_4$ and PVA were improved for efficient photocatalytic removal of major water pollutants. After 140 min, 91.3% of the reactive yellow dye was removed with an optimum band gap of 2.03 eV for the BiVO$_4$/PVA (1 : 3) sample. It has been determined that BiVO$_4$/PVA (1 : 3) has a significant influence on the recombination rate of the photogenerated electron/hole pairs; hence, it decreases the band gap. Recyclability and trapping tests have also been carried out for the stability of the optimized catalyst. This photocatalyst BiVO$_4$/PVA (1 : 3) stable for seven cycles for reactive yellow dye degradation may lead to a world of new production. Other studies will also be performed on its antimicrobial activity, such as through the nanocomposite size, and how it may affect the deactivation of microorganisms. In the antimicrobial activity test, it was shown that the nanocomposites possessed complementary effects in their antibacterial efficacy towards *Escherichia coli* and *Staphylococcus aureus*.

1 Introduction

Water is the most valuable renewable resource after air. Although water covers most of the surface of the earth, only a small portion is exploitable, making it a scarce resource. This precious and rare resource requires careful management. When using water for various purposes, it's important to ensure it is suitable for intended use. Regular monitoring of water sources is crucial to ensure public health.[1] Water is the most scarce resource on Earth, and it is being polluted due to increasing development and population growth, releasing heavy metals, viruses, pesticides, and a variety of organic and inorganic elements. Contaminants offer several environmental and health hazards, complicating the implementation of traditional treatment procedures.[2] Pest control products, medicines, inorganic substances, toxic substances, and colorants for textiles are all examples of pollutants that can have an impact on human well-being and cause illness. Being exposed to these contaminants can also lead to kidney damage, breathing issues, skin cancer, and heart failure. Maintaining a healthy habitat is critical for the survival of aquatic flora and fauna populations.[3] Since World War II, scientists have discovered various pollutants that exhibit hazardous properties and are bioaccumulative, susceptible to long-range transport and persistent in the environment, and even tenacious in the surroundings. They also contribute to major health problems in humans, wildlife, flora, and aquatic ecosystems both near and far from emission source. These harmful pollutants are known as persistent organic pollutants. These are substantially more dangerous than other compounds, despite their smaller quantities.[4] The rise of industrial revolution lead to widespread use of coloring substances, such as colorants, which became increasingly prevalent. These colorants are organically and physiologically stable, and they highly persistent in the environment. Various industries, including textiles, leather, food, cosmetics, paper, and pharmaceuticals, various synthetic dyes. Of these sectors, textiles are the major consumers of dying materials and pigments, and they contribute a substantial volume of effluents following the dying process.[5] Regarding the

[a]Department of Physics, Faculty of Science, University of Gujrat, Hafiz Hayat Campus, Gujrat, 50700, Pakistan. E-mail: sabahshazadii1478@gmail.com; tahir.awan@uog.edu.pk

[b]Department of Zoology, Faculty of Science, University of Gujrat, Hafiz Hayat Campus, Gujrat, 50700, Pakistan

[c]Department of Botany and Microbiology, College of Science, King Saud University, P.O. 2455, Riyadh 11451, Saudi Arabia

[d]Department of Mathematics and Physics, Nanotechnology University of Salento, 73100 Lecce, Italy. E-mail: Zain.ashfaq@unisalento.it

[e]Department of Physics, Faculty of Science, King Khalid University, Abha, Saudi Arabia

† Authors contributed equally.

numerous industries, it is assumed that pharmaceuticals account for 22% of the overall industrial consumption of freshwater, practice has resulted in widespread presence of active medicinal compounds in the aquatic environment.[6] Reactive yellow dyes, like reactive yellow 145, particularly based on azo compounds, are very common in the textile industry, but at the same time, they are very risky in terms of the environment and health. The main feature of these dyes is high stability which makes them resist biodegradation, thus they become non-biodegradable and heavily present in both wastewater and natural ecosystems. Their discharge into water bodies is the main cause of disturbing the natural ecosystem as the water becomes dark and reduces light penetration, as well as disrupts aquatic photosynthesis, which in turn leads to eutrophication of water. Additionally, there are also hazardous dyes' degradation products (*e.g.* aromatic amines) which are both potential mutagens and carcinogens and hence could lead to some health effects of man such as cancer and neurological dysfunctions.[7,8] Conventional methods of treating wastewater, including activated sludge, adsorption, and chemical coagulation, have been utilized for removing pollutants. However, these methods have drawbacks, including expensive maintenance.[9] Reduction using semiconductor photo catalysis technology is a fairly recent method for removing or recovering dispersed metal ions in sewage. This technique uses low-energy UV light and semiconductor particles as a catalyst to generate photo generated electrons.[10] When radiation contacts a semiconductor with a bandgap (E_g) around or below the energy of light, electrons (e^-) in the valence band are driven to the conduction band, resulting in free holes (h^+). According to the energy level of the band edges, excited electrons and holes may combine with water or oxygen molecules to form reactive oxygen species (ROS), such as the radicals hydroxyl ($^{\bullet}OH$) and superoxide radical ($^{\bullet}O^2$), which can break down pollutants.[11] Semiconductor photocatalysts are known for being durable, affordable prices, low ecological impact, super-hydrophilicity, and excellent chemical and photochemical stability[12],[13]. It is utilized extensively in a range of applications, such as detectors, biosensors, solar power devices, catalysis, biological medicine, and energy storage systems.[14] BiVO$_4$ is attractive due to its narrow energy bandgap (2.4–2.5 eV) and optimal band edge sites for the oxygen evolution reaction (OER) from water splitting. Nevertheless, its solar-to-energy conversion capacity has been hampered by low carrier mobility and rapid electron–hole recombination.[15] Bismuth vanadate (BiVO$_4$) is a yellow crystalline solid that is currently gaining prominence as a nanocatalyst. BiVO$_4$ exhibit polymorphism with pucherite (which has a reddish/yellowish brown color with an orthorhombic crystal system), clinobisvanite and dreyerite being about its known polymorphs.[16] BiVO$_4$ stands out for its unique electrical band structure, which includes a Bi 6 s2 lone pair that bends the polyhedron.[17] The tetragonal phase exhibit ultraviolet absorption band, whereas the monoclinic phase absorbs in both the visible and ultraviolet regions.[18] Coprecipitation is a convenient procedure for producing nanoparticles. Coprecipitation can produce a variety of nanoparticles, including metal oxides, magnetic particles, and quantum dots. It is an adaptable

strategy. The dimension and form of the nanoparticles can be organized by modifying constraints such as temperature, pH, and chemical concentrations.[19] Nano-based composites have proven effective at eliminating contaminants from both water and the air.[20] PVA is a semi-crystalline or linear synthetic polymer that is bland, scentless, harmless, biodegradable, and thermally stable. It can be granular or powdered.[21] Polyvinyl alcohol (PVA) with an economical, hydrophilic nature, the ability to degrade water-solubility and useful thermal, chemical, and mechanical strength can be utilized to create water treatment barriers that are very resistant to clogging and have excellent nanofiltration efficiency. Polyvinyl alcohol is synthesized through the hydrolysis of polyvinyl acetate and is often blended with other polymers due to its film-forming features. PVA's physical properties (density, crystallinity, layer formation, solubility in water, volume per mole, and degree of polymerization) differ based on breakdown, crystalline precipitation, molecular mass, and humidity.[22] A composite material comprises at least two chemically or physically distinct phases (structure and dispersion) that display notable bulk traits. Distinct from that ingredient when provided alone. Composites have a constant solid phase that is more flexible than hard. It sustains and distributes burdens with the scattered phase. The secondary phase is the dispersed phase, also known as reinforcement.[23] The BiVO$_4$/PVA composite is a product that coordinates polyvinyl alcohol (PVA) and bismuth vanadate (BiVO$_4$) to promote the processes of water treatment with the aid of visible light radiation of the photo catalysis nature. The BiVO$_4$ semiconductor works well in the degradation of organic pollutants under visible light irradiation with a band gap of 2.3–2.4 eV that is responsible for more efficient oxidation and reduction reactions. Besides, PVA as the binder and a matrix of structure enhances the dispersibility and stability of BiVO$_4$ particles.

The current study contributes a good deal to the overall knowledge in the context of environmental purification due to the introduction of a new BiVO$_4$/PVA nanocomposite with a high level of photocatalytic activity, exceptional stability of performance, and a unique antimicrobial action when compared to the BiVO$_4$-based substances that have already been reported. In terms of photocatalytic degradation capacity and reaction rates, this experiment recorded an outstanding 91.3% removal of reactive yellow dye in only 140 minutes exhibited by the BiVO$_4$/PVA (1 : 3) composite. The performance is significantly high in comparison with other studies. An example is with Karunakaran *et al.* who only achieved a 180-minute reduction in Congo Red dye by about 60% through their synthesized BiVO$_4$. In a similar management, Sari *et al.* degraded 85.34 percent of methylene blue, yet the degradation process took an enormous 240 minutes when compared to the current process. Such rapid, high-yield degradation as described in this paper, thus, constitutes a good enhancement in both kinetics and total effectiveness of the dyes removal. Moreover, operational stability and reusability of the photocatalyst are also very important to practical applications. Although most recent work is concerned with degradation rates at the beginning, the long-term sustainability is quite

Table 1 Comparison of performance between present study and other findings

Nanocomposite	Pollutant	Degradation percentage (%)	References
PVA/BiVO$_4$	Reactive yellow dye	91.3% in 140 minutes	Our findings
Au/BiVO$_4$	MO dye	78% in 8 hours	https://doi.org/10.1016/j.jallcom.2009.11.027
Co-BiVO$_4$ composites	MB dye	85% in 5 hours	https://doi.org/10.1016/j.apcatb.2010.06.022
BiVO$_4$/BiOCl composites	Rhodamine B (RhB)	85% in 180 minutes	https://doi.org/10.1016/j.seppur.2016.10.010
rGO/Bi$_2$WO$_6$	Norfloxacin	87.49% in 180 hours	https://doi.org/10.1016/j.jcis.2021.01.016
Ag/BiVO$_4$	MO dye	75% in 240 minutes	https://doi.org/10.1016/j.apsusc.2009.12.009
Cu/BiVO$_4$	Rhodamine B (RhB)	87% in 210 minutes	https://doi.org/10.1007/s10854-015-4037-5
BiVO$_4$-graphene nanocomposites	Rhodamine B (RhB)	87% in 20 hours	https://doi.org/10.1155/2014/401697

problematic. In this study, the high performance of BiVO$_4$/PVA (1 : 3) composite was clearly emphasized with a seven-consecutive cycle activity measurement during the reactive yellow dye degradation. The extreme and impressive tests that are performed on the field of stability can offer very convincing argument of the lasting quality of the material, something which seems to be left in the shadow or rather hardly accomplished in the comparable works. More importantly, an added and equally interesting aspect of the usefulness of the material is also revealed in the manuscript concerning the antimicrobial activity of the material. Though the aforementioned studies, many of which have center their focus entirely on photocatalytic degradation of chemical pollutants, the present study clearly states that it has observed complementary effects on bacterial killing of *Escherichia coli* and *Staphylococcus aureus*. This two-fold effect that is there at the same time fouling the water with chemical colored dye and cleaning it of microbial contamination makes the BiVO$_4$/PVA nanocomposite a more well-rounded and functional water-purifying material than a narrowly focused photocatalyst that fights one possible form of water pollution.

The current study under consideration contributes to the subject considerably, especially due to the high effectiveness with regard to the reactive yellow dye removal and the antimicrobial properties discovered, which represents a strong case of a dual-purpose. Following this, the opportunities of real-world incorporation are larger, with the main potential set on conversion of the powder into useful shapes such as functional composites and films. This would open the possibility of use in application like continuous flow photocatalytic reactors in industrial wastewater treatment as well as application in self-disinfecting surfaces, beyond the restrictions of batch-wise applications of powder. Nevertheless, there is still much work to be done along the way such as the development of efficient and economical synthetic procedures to make large volume materials, and the durability of the materials throughout various conditions *via* the integration of the materials and their assurance in the real world with complex effluent conditions, which would still define robust translational research.

A novel nanocomposite was synthesized for this study and employed as a photo catalyst using a simple coprecipitation approach. For the efficient breakdown of reactive yellow dye, the produced photo catalyst is employed. To investigate the structural properties of the synthesized catalyst, SEM and X-ray diffraction (XRD) were employed. UV, PL, and FTIR spectroscopy have been employed to examine the optical and electrical characteristics. In this novel study we employ the produced photo catalyst to examine the antibacterial and antimicrobial activity (Table 1).

2 Experimental methodology

2.1. Materials and reagents

Chemicals utilized in composite synthesis include bismuth nitrate pentahydrate Bi(NO$_3$)$_3$·5H$_2$O, distilled (DI)water, ammonium meta vanadate NH$_4$VO$_3$, sodium hydroxide NaOH, and polyvinyl alcohol (PVA), which were self-prepared in the Nanotechnology Lab at the University of Gujarat. Each of the experimental reagents and compounds used in this work were donated by Sigma Aldrich, and none had been purified before being utilized.

2.2. Synthesis of pure BiVO$_4$

Pure BiVO$_4$ nanostructures were synthesized by a straightforward coprecipitation technique. There were two aqueous solutions created at 70 °C. The first solution A involves dissolving 4 g of Bi (NO$_3$)$_3$·5H$_2$O in 40 ml of distilled water. For the second solution B 40 ml of distilled water was utilized to dissolve 1.28 g of NH$_4$VO$_3$. With vigorous stirring, solution A was added drop by drop to Solution B and then 5 g of sodium hydroxide was dissolved in 35 ml distilled water separately to increase the pH value up to 9, NaOH solution was constantly added drop by drop into the above solution with continuous stirring for 1 hour. To ensure the elimination of surface-bound contaminants, the light yellowish solution was cleansed using distilled water and pure ethanol. After being dried in an oven for a full day, the precipitate eventually grained. In a muffle furnace, this BiVO$_4$ powder was calcined for one hour at 400 °C. The material was calcined and then let it cool down to ambient temperature before being firmly mashed with a mortar and pestle. At last, pure BiVO$_4$ NPs were produced (Fig. 1).

2.3. Synthesis of BiVO$_4$/PVA

The BiVO$_4$/PVA (1 : 1) composite was synthesized by mixing 1.95 g of PVA in 40 ml of distilled water (Solution A) and 1.25 g of BiVO$_4$ in 40 ml of distilled water (Solution B). Solution A was then poured into Solution B under continuous stirring. A sodium hydroxide solution is prepared by dissolving 5 g of NaOH in 30 ml
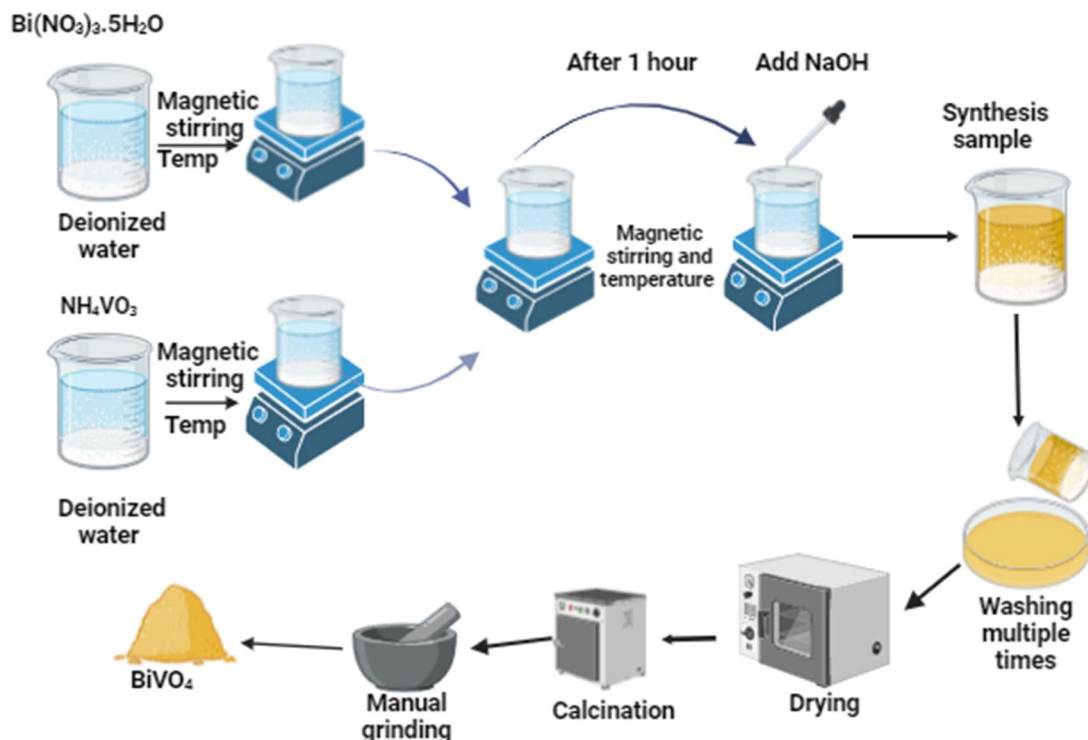
Fig. 1   The schematic diagram of the synthesis of BiVO$_4$ nanoparticles.

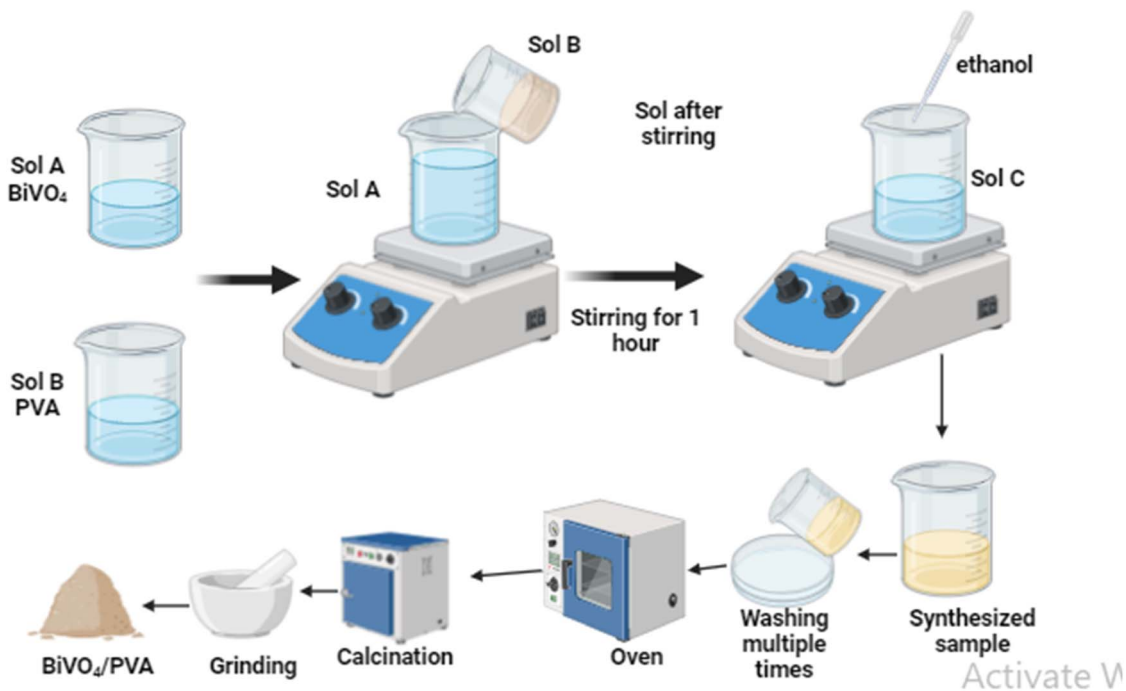Fig. 2   The schematic diagram of the synthesis of BiVO$_4$/PVA nanoparticles.

of distilled water, was added dropwise to the mixture while stirring. The stirring of the mixed solution was done for 180 minutes to make the solution uniform. The obtained product was thoroughly washed with ethanol and distilled water, then dried at 60 °C for 15 hours and calcined in a muffle furnace at 500 °C for 2

hours. A light yellow powder was yielded. The BiVO$_4$/PVA (1 : 2) and BiVO$_4$/PVA (1 : 3) composites were similarly synthesized by varying the quantity of BiVO$_4$ in Solution B (1.35 g for the BiVO$_4$/ PVA (1 : 2) and 1.46 g BiVO$_4$/PVA (1 : 3) while maintaining constant proportions of PVA and NaOH (Fig. 2).

2.4. Material characterization

The X-ray diffraction (XRD) approach is utilized to analyze the crystal structure of nanoparticles with an average particle dimension. FTIR spectra allow for the recognition of unknown materials. The optical properties of a substance are investigated using ultraviolet-visible spectroscopy. Photoluminescence spectroscopy allows us to analyze the electrical characteristics of diverse materials. A scanning electron microscope (SEM) produces a high-resolution, expanded image.

3 Results and discussions

3.1. UV-vis spectroscopy

UV-vis double-beam spectrometry was utilized to examine the absorption spectrum of the synthesized nano composites. For evaluating the absorption of $BiVO_4$/PVA composites, before pouring the fine powder in the cuvette, dilute it in ethanol and sonicate it. Thus, to investigate the optical characteristics the tauc illustration is based on absorption mode. Absorption is assessed as an indicator of wavelength, which ranges from 455 to 800 nm. The raised absorbance promotes the excitation of a larger amount of holes as well as electrons *via* UV radiation, hence increasing photocatalytic activity. It is observed that the $BiVO_4$/PVA has the absorption peak at 513 nm. The band gap energy was determined with the Tauc plot [$(\alpha h\nu)^{1/2}$ *vs.* $(h\nu)$]. PVA and $BiVO_4$ nanoparticles have predicted indirect band gaps of 2.7 and 2.4 eV, respectively. As PVA concentration rises, the energy barrier between conduction and valence bands in the $BiVO_4$/PVA nano composite lowers.[24] The band gap of nano composite decreases by varying concentration of PVA due to aggregation. Band gap data show that raising PVA content reduces the band gap, absorbs more visible light, and enhances charge carrier segregation, all of which promote photocatalytic degradation of Reactive yellow. The band gap values of $BiVO_4$/PVA (1 : 1), $BiVO_4$/PVA (1 : 2) and $BiVO_4$/PVA (1 : 3) were 2.3, 2.18, and 2.0 eV respectively for indirect transition. Because the

synthesized substance is not always an enduring compound, UV-visible spectroscopy might generate some noise.[25] The band gap energy is investigated employing the formula (Fig. 3).

$$\alpha h\nu = A(h\nu - E_g)^n \tag{i}$$

Here "h" stands for the Planck constant, "ν" for photon frequency, and "E_g" for band gap energy.

3.2. Photoluminescence spectroscopy

The flaws of the material were identified using photoluminescence spectroscopy (PL: RAMANLOG 6, UOG). Enhanced PL intensity is commonly employed to describe the maximal rate of photogenerated electron and hole's pair recombination in materials. The relocation, movement, and confinement of photogenerated electron–hole pairs in PVA has
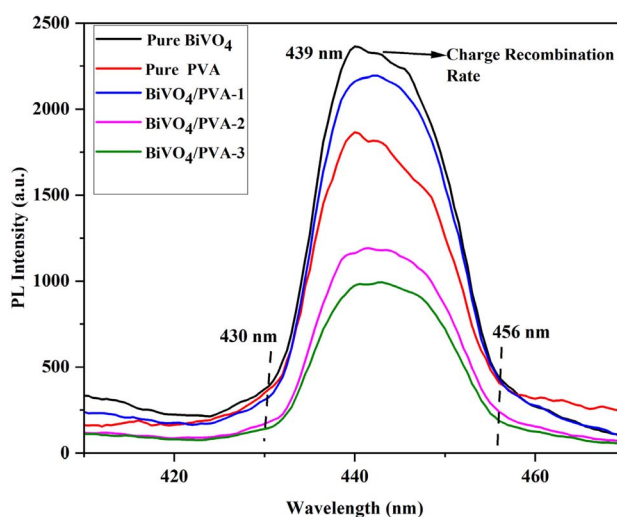

Fig. 4 PL spectra of pure $BiVO_4$, PVA, $BiVO_4$/PVA (1 : 1), $BiVO_4$/PVA (1 : 2) & $BiVO_4$/PVA (1 : 3).

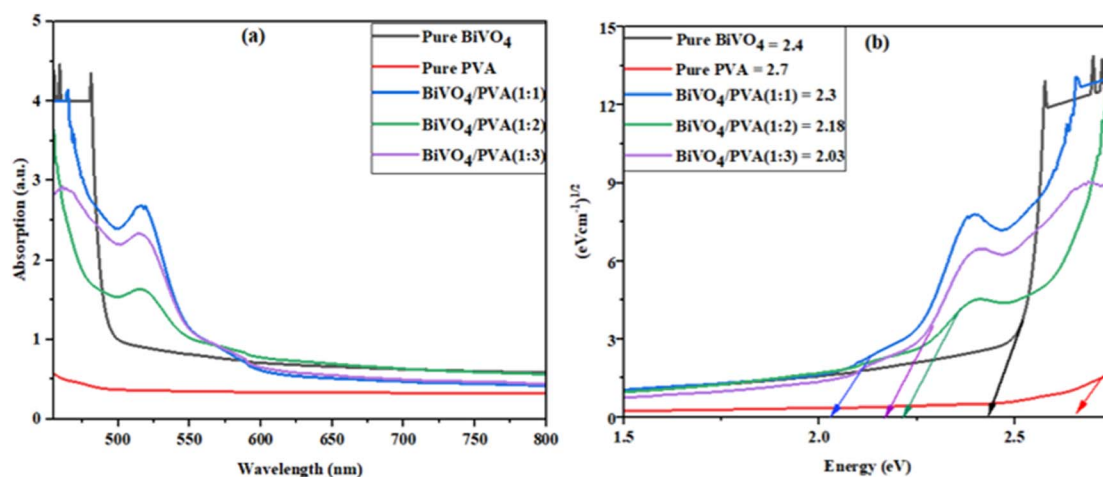**Fig. 3** UV-vis spectra of pure $BiVO_4$, PVA, $BiVO_4$/PVA (1 : 1), $BiVO_4$/PVA (1 : 2), & $BiVO_4$/PVA (1 : 3), (a) absorption spectra (b) Tauc plot to determine the indirect band gap of synthesized materials.
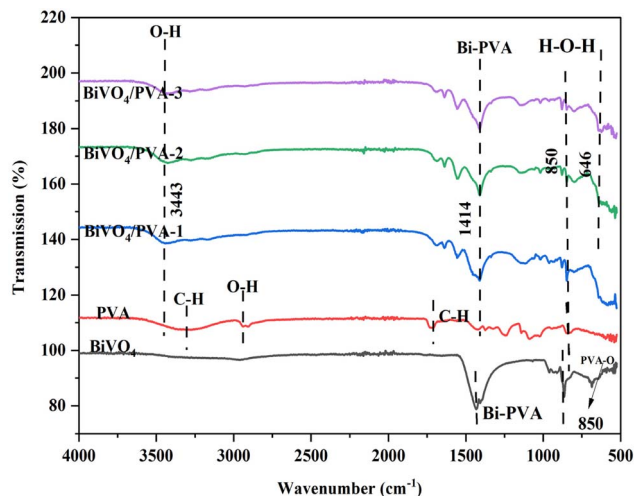
Fig. 5 FTIR spectra of pure $BiVO_4$, PVA, $BiVO_4$/PVA (1 : 1), $BiVO_4$/PVA (1 : 2) & $BiVO_4$/PVA (1 : 3).

been investigated using photoluminescence (PL) techniques. The excitation wavelength for this technique is 400 nm. A reduction in photoluminescence intensity typically enhances the effectiveness of photo induced charge separation, which in turn leads to a rise in photocatalytic activity. The peak at 439 nm indicates high charger recombination rates for photogenerated electron–hole pairs, but low photocatalytic efficiency.[26] The $BiVO_4$/PVA (1 : 3) composite reduces the PL emission spectrum significantly compared to pristine PVA and $BiVO_4$, which have large intensity peaks and low photocatalytic efficiency. The peak at 430 nm depicts the band gap of nanocomposites. The $BiVO_4$/ PVA (1 : 3) generates the highest duration delay in the

recombination of generated charge carriers, leading to the most significant deterioration of Reactive yellow. It has also been revealed that some faults put into the material at 456 nm result in dislocation production.[27] The passage of holes in PVA will result in a substantial decrease in the degree of recombination of photogenerated charge carriers, and the composites give a new defect site that may significantly reduce the electrons imprisoned in oxygen-free spaces (Fig. 4).

3.3. Fourier transform infrared spectroscopy

To examine the functional groups associated with these PVA/ $BiVO_4$ nanocomposite materials, FTIR spectroscopy is utilized. All synthesized composites are projected to have peak absorption rates in the 400–4000 cm^{-1} range, as indicated in the figure. The sharp peaks were detected at 646 cm^{-1}, 850 cm^{-1} 1414 cm^{-1}, and 3443 cm^{-1}. The black spectrum is indicative of inorganic vibration at frequency lower than 850 cm^{-1}. The red spectrum reveals main bonds for O–H stretching at 3443 cm^{-1} (ref. 28), and C–H stretching at 3304 cm^{-1} (ref. 29), O–H bending at 2946 cm^{-1} and C–O stretching at 1040 cm^{-1} (ref. 30). The top three spectra of composites show common features of both pure components which confirms that the composites have been formed successfully. The material is pure PVA aas indicated by presence of bonds of O–H, C–H, and C–O, while bonds below 850 cm^{-1} is characteristics of pure BiVO4. The main cause of changes in PVA and $BiVO_4$ is interaction of hydrogen bonds that are formed between hydroxyl group (−OH) of PVA and oxygen species on surface of $BiVO_4$. This hydrogen bonding can be seen from small shifts and increase in Vibration peak of O–H at 3443 cm^{-1} in composite spectra with respect to pure PVA The bending peak at 646 cm^{-1} indicate the presence of PVA-O bond.[31] The stretching peak were observed at 850 cm^{-1}
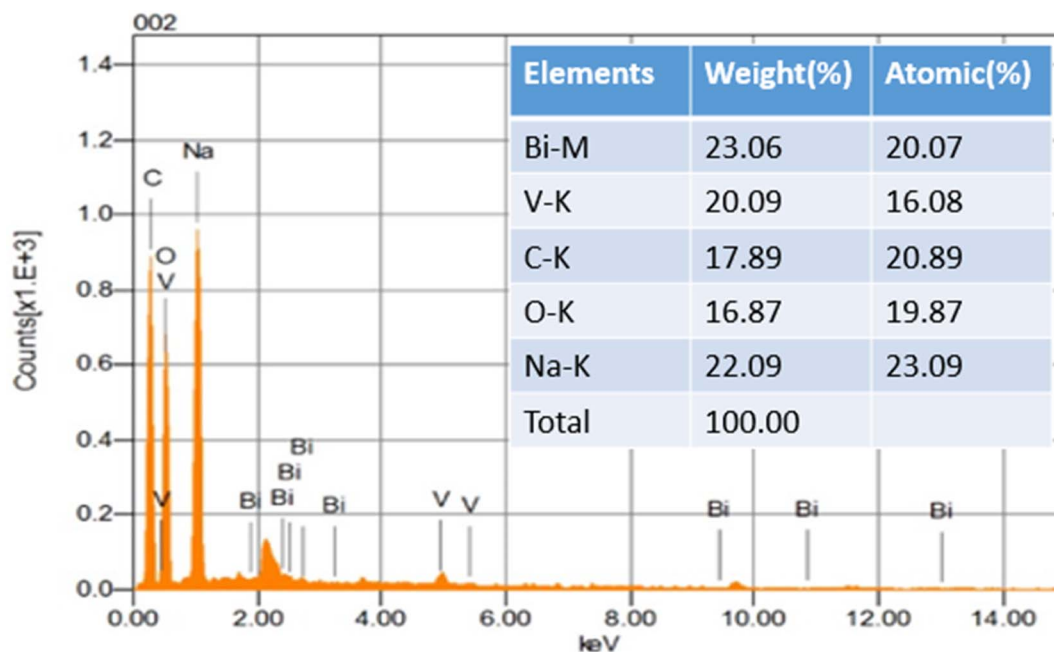

Fig. 6 The EDX analysis of $BiVO_4$/PVA (1 : 3).

and 1414 cm^{-1} indicate the involvement of H–O–H and Bi-PVA bond (Fig. 5).

3.4. Energy dispersive spectroscopy(EDS)

EDX were performed on BiVO$_4$/PVA (1 : 3) to check the elemental composition of nano composites both quantitatively and qualitatively.[32] The EDX analysis reveal that there is no impurity in the sample. The pure BiVO$_4$ is composed of bismuth, vanadium and oxygen, while the PVA is made up of hydrogen, oxygen and hydroxide ion. Since the hydrogen is the lightest element so its peak does not occur in EDX analysis. The carbon peak is due to the placement of sample in carbon tape. The high sodium peak is due to the use of sodium hydroxide to maintain pH (Fig. 6).

3.5. SEM morphology

SEM images of pure BiVO$_4$, pure PVA, and BiVO$_4$/PVA (1 : 3) with different magnifications are depicted in Fig. 7(a)–(d). The pure BiVO$_4$ has the predominantly rod like shape at 0.5 μm as

illustrated in figure (a). The pure PVA has an irregular nano-cluster at 2 μm as shown in figure (b). Figures (c) and (d) illustrate that the BiVO$_4$/PVA (1 : 3) has three dimensional agglomoration of irregular shaped nanoparticles at the resolution of 2 μm and collection of exfoliated nanosheets at the resolution of 5 μm. The pure BiVO$_4$ has a crystalline size of 71 nm. The BiVO$_4$/PVA (1 : 3) nanocomposite exhibited an average particle size of 30 nm as in (Fig. 8), confirming the formation of relatively uniform nanostructures. The exfoliated nanosheets as in Fig. 7(d) are significant for providing a very high specific surface area that basically ensures maximum active sites for reactant adsorption as well as light absorption. At the same time, the decreased mean particle size of the BiVO$_4$/PVA (1 : 3) composite additionally contributes to the surface area and improves the light absorption capacity of the material. The three-dimensional agglomeration of the irregular nano-particles in Fig. 7(c), when it is in control, can actually help in creating a porous network which further enables light trapping and scattering, thus providing more efficient use of the
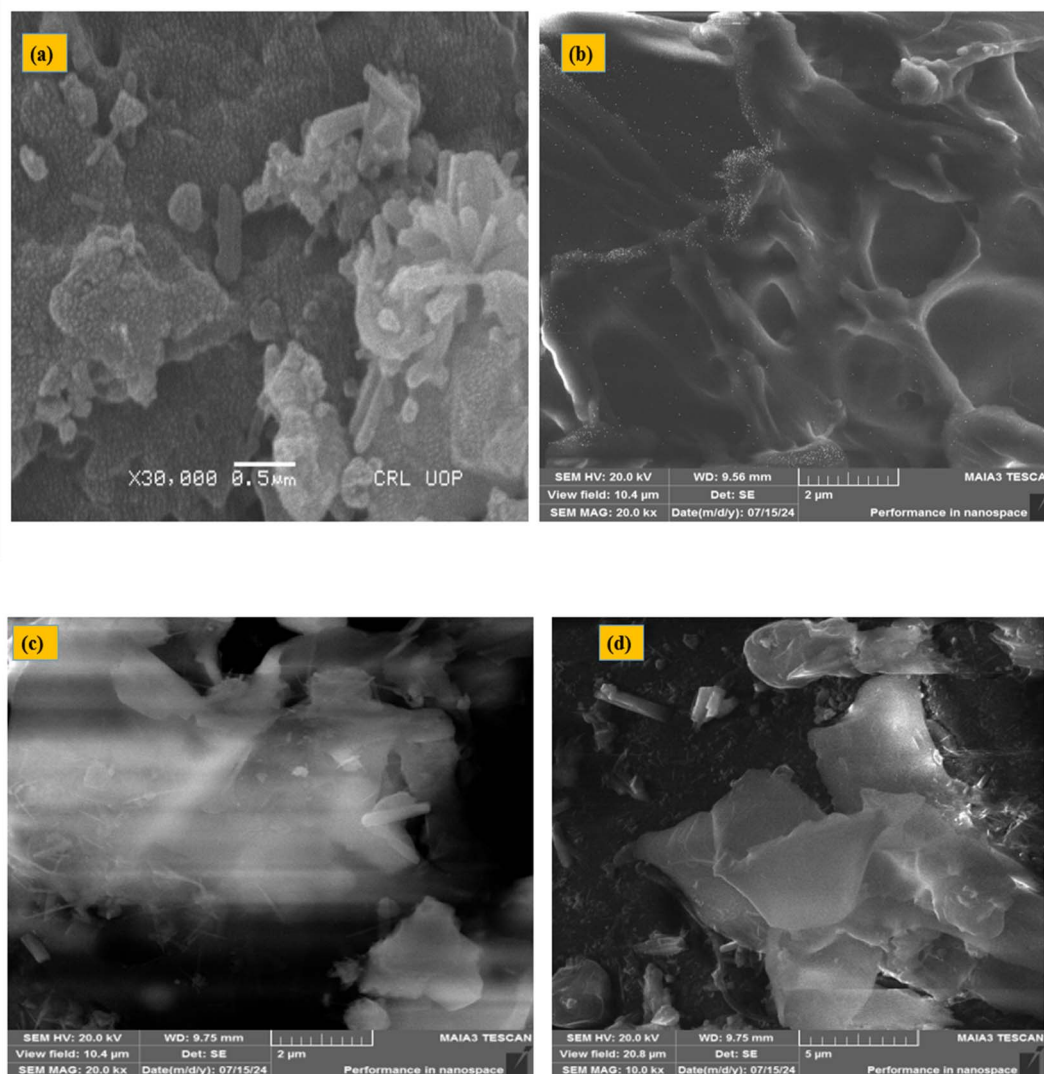

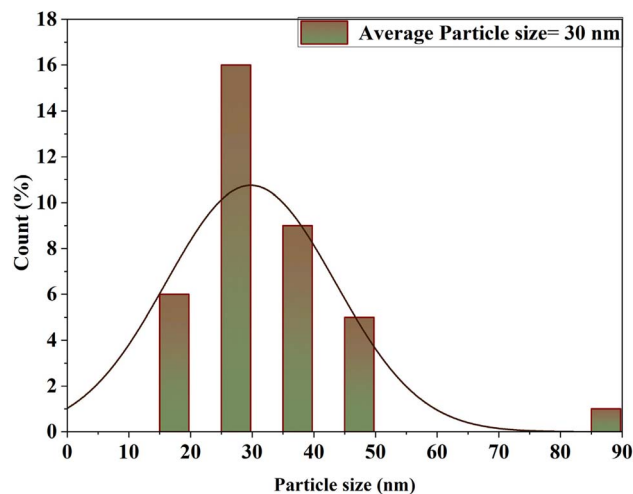Fig. 7 (a) Is pure BiVO$_4$, (b) is pure PVA (c) and (d) is BiVO$_4$/PVA (1 : 3) at different resolution.

Fig. 8 Illustrate the particle size histogram of BiVO$_4$/PVA (1 : 3) nanocomposite.

photons. This special combination of high surface area, better light harvesting along with the possibility of the charge separation improvement at the BiVO4/PVA (1 : 3) nanocomposite, in effect, becomes the major factors that lead to the superior photocatalytic performance of reactive yellow dye. The particle size histogram of BiVO$_4$/PVA (1 : 3) nanocomposite is now presented as a new panel in (Fig. 8).

3.6. XRD analysis

The X-ray Diffraction pattern of a BiVO$_4$ with no impurities has clearly defined diffraction peaks that match the card #00-044-0429 from the JCPDS library, which are the characteristic features of a highly crystalline nature with a cubic phase. The purity of the phase is inferred from the lack of any peaks attributed to foreign substances. The highest intensity peak that we observe is due to the (310) plane, displaying great crystallite size and low microstrain by the sharpness of the peak. The pure

PVA has the lattice parameters $a = 10.2180$, $b = 10.4010$, $c = 5.6710$, and $\alpha = \beta = \gamma = 90$. Lattice parameters for the BiVO$_4$/PVA (1 : 2) are $a = 6.9820$, $b = 6.9820$, $c = 6.4764$ and $\alpha = \beta = 90$ and $\gamma = 120$ and its density is 5.54 g cm^{-3} (JCPDS#00-015-0766). Lattice parameters for the BiVO$_4$/PVA (1 : 3) are $a = 18.8000$, $b = 18.8000$, $c = 18.8000$, and $\alpha = \beta = \gamma = 90$ associated with cubic phase. The material undergoes certain dehydration upon annealing at the temperature of 400 Celsius which results in the formation of a cubic phase for pure BiVO$_4$. As the annealing temperature is increased the cubic phase is transformed into hexagonal for BiVO$_4$/PVA (1 : 2). But as the concentration varies the effect of annealing temperature changes its shift to cubic phase as in BiVO$_4$/PVA (1 : 3).[33] The Scherrer formula is used to investigate the average crystalline size (Fig. 9)

$$D = 0.89\lambda/\beta \quad \cos \quad \theta \qquad (ii)$$

where λ is the measurement of radiation wavelength and D is the measurment of the crystallite size and β is measurment of FWHM in the radians and θ represent the diffraction angle. The pure BiVO$_4$ has the crystallite size of 53 nm. As by varying concentration the crystallite size decreases.

4 Photocatalytic activity

4.1. Photocatalytic activity for reactive yellow dye

A photocatalytic reactor from the Nanotechnology Laboratory, Department of Physics, University of Gujrat, Pakistan, was employed to break down the reactive yellow dye. A 450 W high-pressure mercury lamp was used to irradiate the photo catalysts. The separation between the solution and the UV-vis bulb remained constant at 16 cm. A gap of 12–20 cm is recommended separating the reaction solution and irradiation source. The pollutant solution was prepared by dissolving 0.01 g of reactive yellow dye in 500 ml distilled water and stirr the solution for 20 minutes in the complete darkness. A UV-visible spectrophotometer has been employed to test absorbance over 200–900 nm wavelengths. The light absorption was measured
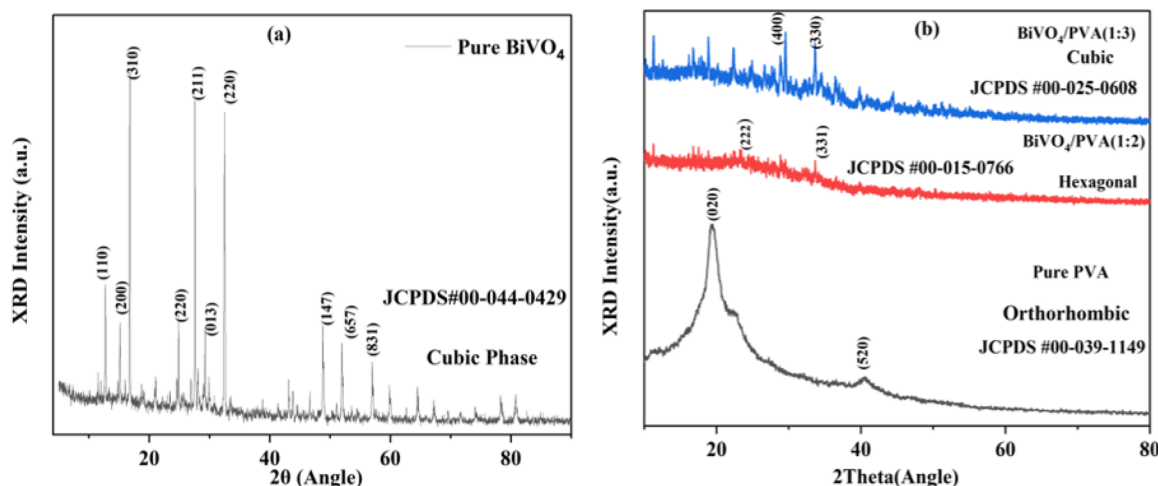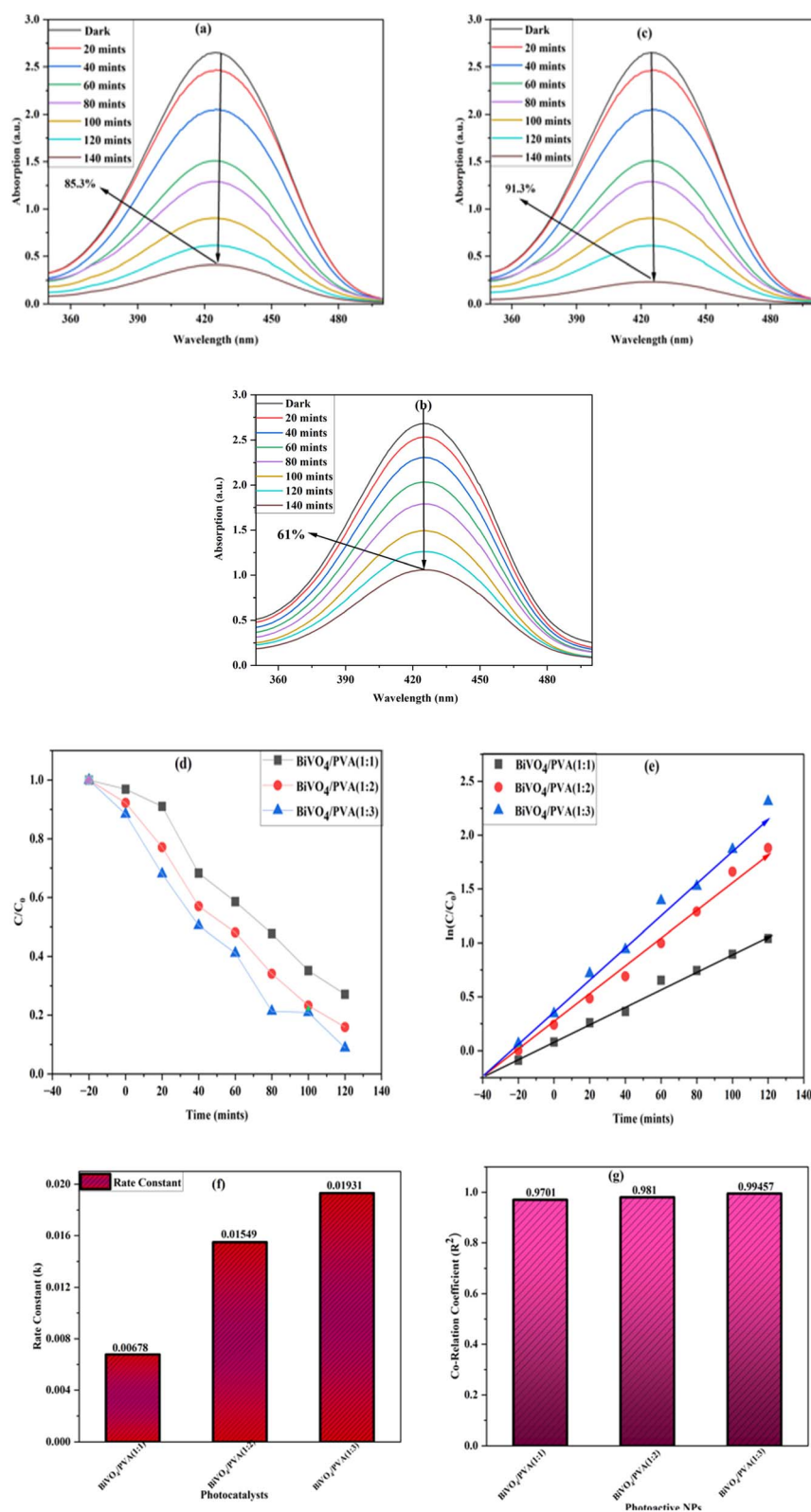

Fig. 9 XRD analysis of (a) pure BiVO$_4$ (ref. 34), b) pure PVA and BiVO$_4$/PVA (1 : 2) & BiVO$_4$/PVA (1 : 3).

Fig. 10 (a) Represent the photocatalytic activity of BiVO$_4$/PVA (1 : 1) at 140 minutes, (b) represent the photocatalytic activity PVA at 140 minutes, (c) represent the photocatalytic activity of BiVO$_4$/PVA (1 : 3) at 140 minutes (d and e) represents the degradation constants and first order kinetics of the reactions for BiVO$_4$/PVA (1 : 1), BiVO$_4$/PVA (1 : 2), BiVO$_4$/PVA (1 : 3) (f and g) represent the rate constant and correlation coefficient of BiVO$_4$/PVA (1 : 1), BiVO$_4$/PVA (1 : 2), BiVO$_4$/PVA (1 : 3).

using a UV-vis spectrophotometer and extracted. Bring a 5 ml solutions out of the beaker. A further 0.02 g of the BiVO$_4$, PVA BiVO$_4$/PVA (1 : 1)(1 : 2) & (1 : 3) catalyst was each added to 100 ml of reactive yellow dye solution maintaining a pH of 4 at 55 °C. After measuring the photo catalysts, they were placed to simulate pollutant solutions and stirred for 20 minutes in total darkness and take the reading and then places it in photocatalytic reactor. A UV-vis spectrophotometer was used to extract and test 5 milliliters of the contaminated solution to assess dye adsorption in the absence of light.[35] It takes 140 minutes to perform the entire photocatalytic activity. The solutions hue changes from deep yellow to virtually colorless over time. BiVO$_4$/PVA (1 : 3) has the maximum degradation of 91.3%. The photocatalytic activity of nanocomposites was calculated using the formula,

$$D\% = (1 - C/C_0) \times 100 \qquad \text{(iii)}$$

where C_0 represents the initial concentration and C represents the concentration after time t. As time passes, the absorption peaks migrate downward, indicating that the reactive yellow dye is degrading. The BiVO$_4$/PVA (1 : 3) concentration is quite effective at degrading reactive yellow dye. We may also determine the rate constant K and its percentages utilizing photocatalytic activity values. In this phase of the activity, we determine whether or not the activity's results are linear or not.[36] The highest range of estimated rate constant (K) values indicates the maximum degradation efficiency. The BiVO$_4$/PVA (1 : 3) nanocomposites were found to have a maximum rate constant of 0.1931 and a maximum percentage of 91.3% (Fig. 10).

$$\ln(C_0/C) = KT \qquad \text{(iv)}$$

4.2. Cyclic test

The cyclic test of BiVO$_4$/PVA (1 : 3) nanocomposite (NPs) involves continuously testing the nanoparticles to establish their long-term dependability and functionality. This test is crucial for establishing the durability and use of BiVO$_4$/PVA (1 : 3) nano composite in a range of applications, particularly in water splitting by photoelectrochemical methods for wastewater disposal. Cyclic studies enables researchers to evaluate how nanoparticles behave under frequently challenging conditions, yielding conclusions regarding the reliability and potential for practical implementation in sustainable solar water excruciating technology. The cyclic experiment is often supported by repeatedly accomplishment photoelectrochemical measurements on BiVO$_4$ nanoparticles. Each cycle comprises illuminating the NPs and measuring their photocurrent density at an practical power.[37] The NPs then enter a state of passivity in dark until the following series begins. Repetition of these stages allows investigators to understand in what way the photocurrent concentration and further performance characteristics of BiVO$_4$/PVA (1 : 3) nano composite vary over time. This insight gives light on the nanoparticles' resilience and endurance in operating conditions. Following the photochemical experiment,
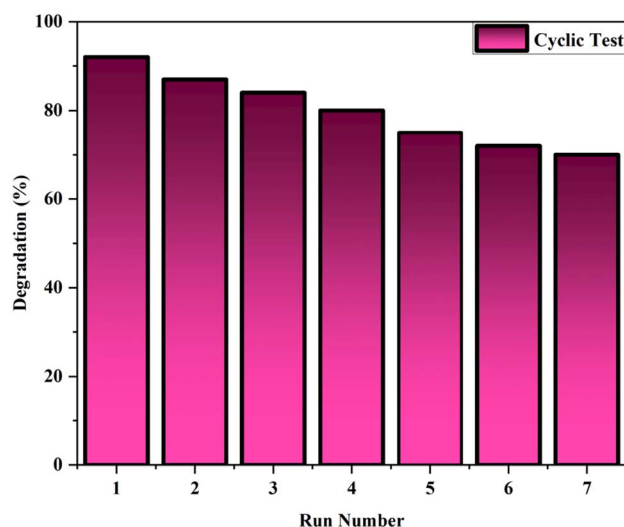

Fig. 11   The cyclic test of optimal sample.

the substrate was periodically cleaned with acetone and water to eliminate any undesirable substances. It was subsequently dried at 500° for four hours before being utilized in the next test. After seven more applications of optimal BiVO$_4$/PVA (1 : 3) for reactive yellow dye degradation, the percentage breakdown of the dye occasioned in just a modest reduction in photocatalytic performance, indicating that the material had enhanced photocatalytic longevity.[38] The results show that photocatalytic efficiency reduces, even though not dramatically. This outcome reduces processing expenses and is advantageous for the disposal and reuse of BiVO$_4$/PVA photocatalyst (Fig. 11).

4.3. Scavengers radical test

The scavenger radical test evaluates compounds' potential to neutralize or eliminate free radicals from a system. This test is very important in sewage treatment since it allows you to evaluate the efficacy of different procedures as well as recognize the reactive substances that cause degradation of contaminants. The scavenger radical test includes introducing a scavenger to the mixture of reactions to determine which reactive species are accountable for pollutant breakdown. For example, IPA trapped hydroxyl radicals, P-BQ traps superoxide radicals, EDTA traps holes, and DMSO traps electrons. Scavenger tests assess the antioxidant capabilities of compounds, which are critical for biological systems protection and nutritional preservation. The scavenger radical test aids in identifying the reactive species that contribute to pollutant breakdown, hence making sure that wastewater treatment operations run efficiently. Various scavengers, such as BQ, methanol, and isopropanol (IPA), have been found to successfully capture superoxide radicals, holes, and hydroxyl radicals generated throughout semiconducting material stimulation.[39] Figure below portrays the variation in reactive yellow level as an indicator of irradiation length in either the presence or the absence of various scavengers, including a BiVO$_4$/PVA (1 : 3) nanocomposite, to help understand the photocatalytic process and the significance of the primary
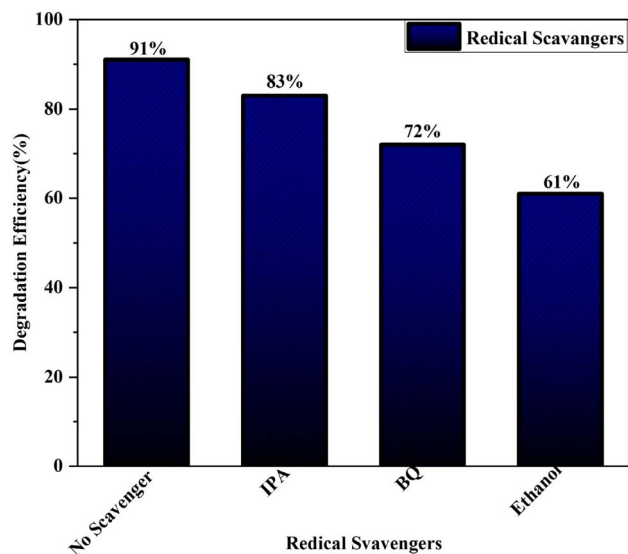
Fig. 12 The Scavenger radical test of an optimal sample.

reactive components involved in photocatalytic degradation. Scavengers like ethanol and IPA can greatly hinder the degradation rate of yellow reactive, showing that superoxide radicals and hydroxyl radicals are the primary reactive components that contribute to degradation (Fig. 12).

4.4. Graphical mechanism of photocatalyst

The addition of $BiVO_4$ to the PVA matrix moves the absorption edge into the visible light region. This is owing to BiVO4's reduced band gap (2.4–2.5 eV) as opposed to pure PVA (4.9 eV). The higher absorption in the visible light band boosts the

nanocomposite's photocatalytic activity. The inclusion of $BiVO_4$ to the PVA polymer lowers the direct band gap from 4.9 eV for pure PVA to around 2.18 eV for the PVA/$BiVO_4$ nanocomposite. This decrease in the band gap enables the nanocomposite to absorb a broader range of visible light, increasing its photocatalytic efficacy. When a photocatalyst substance, such as Bismuth vanadate ($BiVO_4$) is subjected to light energy (usually UV or visible light), an electron in the semiconductor's valence band is stimulated to transfer energy to the conduction band. This produces an electron–hole pair.[40] The electrons in the conduction band oxidize oxygen to make superoxide radicals ($O_2^{\bullet-}$), whereas the holes in the valence band oxidize water or hydroxide ions to form incredibly reactive hydroxyl radicals ($^{\bullet}OH$). Superoxide radicals and hydroxyl radicals are strong oxidizing agents that can degrade organic contaminants into lesser, less hazardous molecules. Organic contaminants are eventually mineralized into CO_2 and water (H_2O) by a succession of oxidation events catalyzed by the produced radicals.[41] The oxidized products disappear from the photocatalyst surface, permitting the cycle to continue (Fig. 13).

5 Antimicrobial activity assessment

The antibacterial activity of synthesized composites underwent evaluation using *Escherichia coli* and *Staphylococcus aureus*. The agar disc diffusion method is a versatile testing methodology that can be employed for assessing antimicrobial substances. The antibacterial activity was performed to control the bacterial growth. This approach was also applied to assess antifungal activity against *Rosellinia necatrix* and Fusarium spp. Fresh colonies were grown using bacterial and fungal growth media,
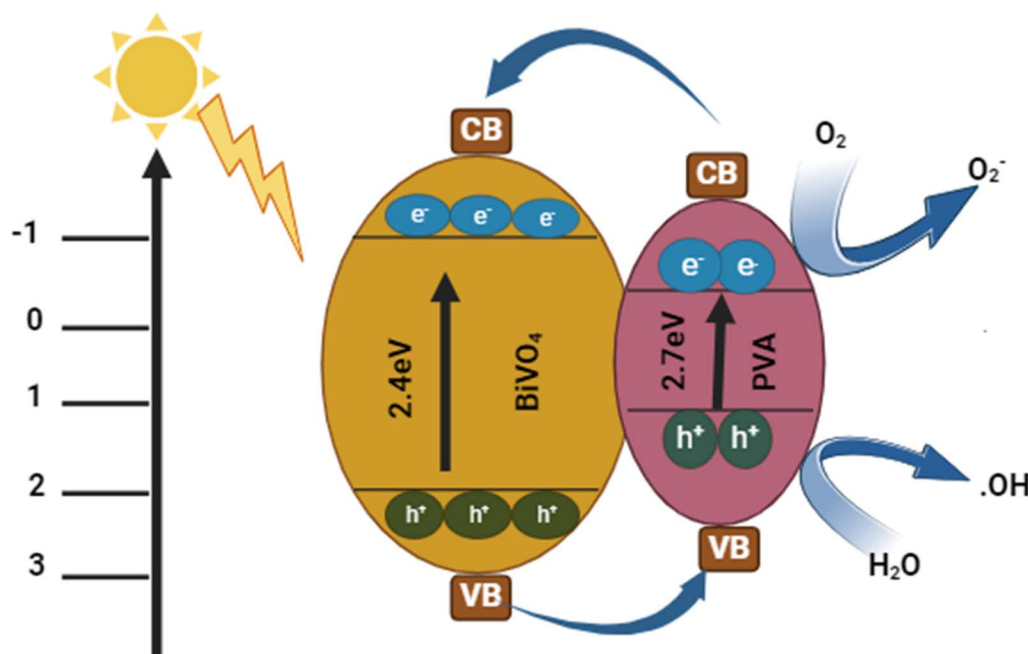

Fig. 13 Represents the graphical mechanism of photocatalysis for nanocomposite.
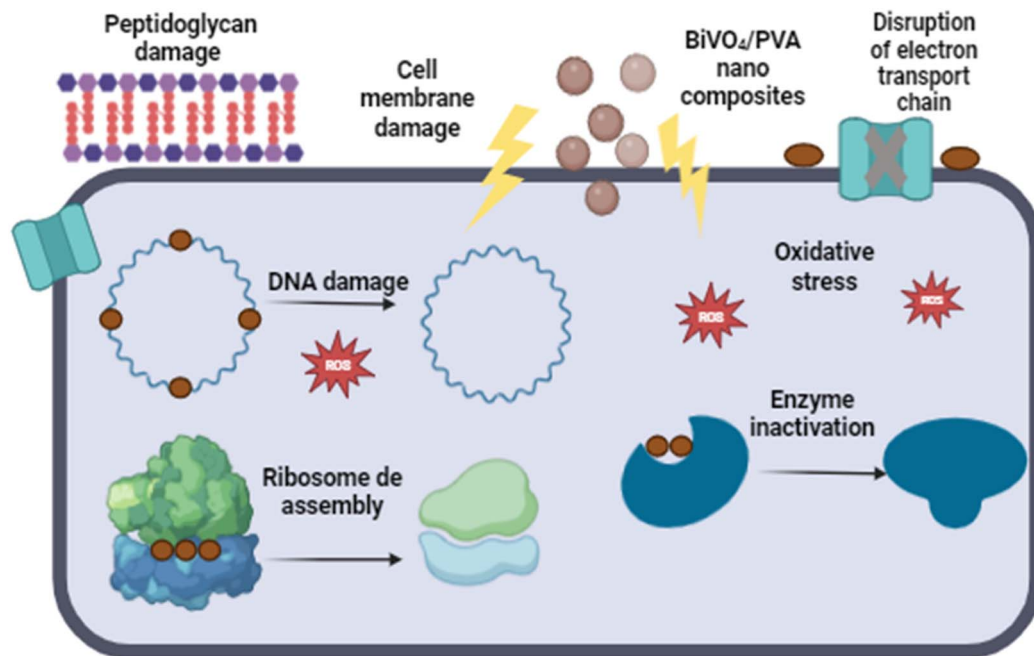
Fig. 14 Graphical mechanism for antimicrobial potential of BiVO$_4$/PVA nanocomposite.

combining nutrition broth and culture media. The antifungal activity were performed to inhibit the growth of fungus (Fig. 14).

5.1. Antimicrobial and antifungal activity

Incorporating BiVO$_4$ nanoparticles into a PVA polymer matrix greatly increased the nanocomposite's antibacterial activity in contrasted with pure PVA or BiVO$_4$ individually. The nanocomposite effectively inhibited bacterial growth, including *Staphylococcus aureus* and *E. coli* strains. Cultivate colonies of the test bacterial strains. Create a suspension of live bacteria in sterile saline or broth and modify its turbidity to match a 0.5 McFarland standard. Distribute sterile Mueller-Hinton agar into the Petri dishes and let it to harden. Use a sterile swab to evenly distribute the bacterial inoculum throughout the surface of the agar plates. Cut or punch discs from the PVA/BiVO$_4$ nanocomposite material. Gently lay the nanocomposite discs on the infected agar plates. Incubate the plates at 35–37 °C for 18–24 hours. Following incubation, estimate the diameter of the clear zones of bacterial development retardation surrounding each nanocomposite disc. The measurement of the inhibition zone represents the antibacterial activity of the nanocomposites.[42] The increased antibacterial activity of the PVA/
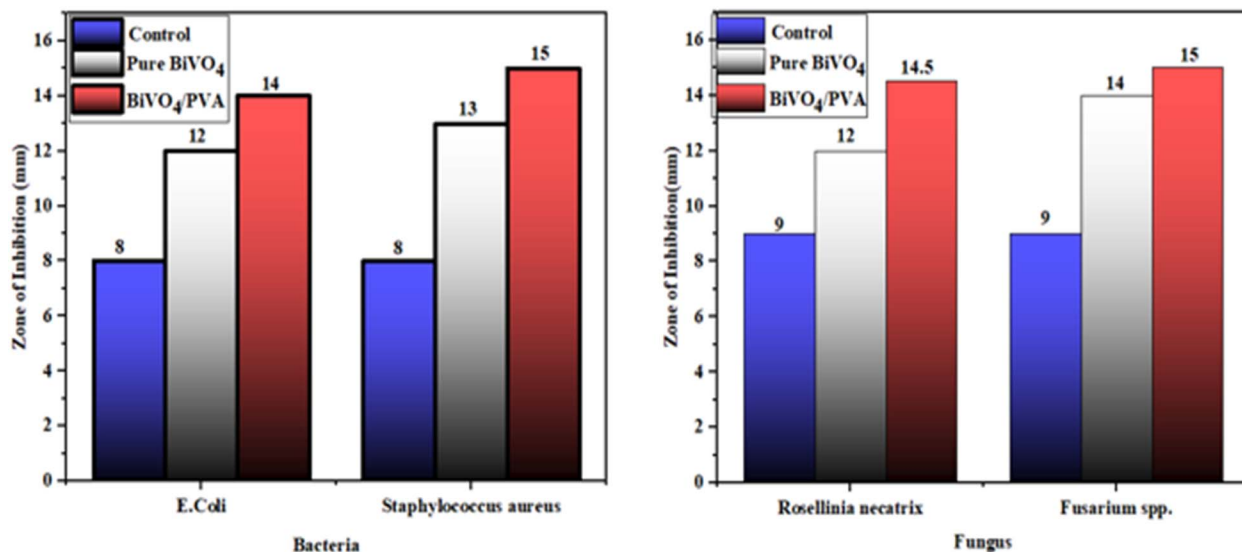

Fig. 15 Represents the antibacterial and antifungal activity of pure BiVO$_4$, BiVO$_4$/PVA.
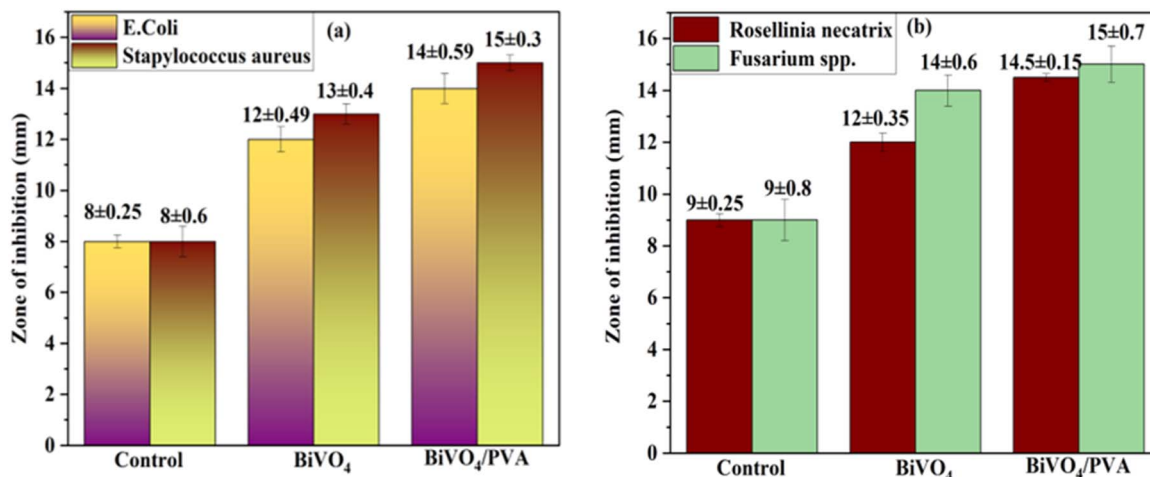
Fig. 16 (a and b) represents the errors bar graph of antibacterial and antifungal activity for control, pure BiVO$_4$ and BiVO$_4$/PVA.

Table 2 Represents the inhibition zone diameter and calculated MIC value of bacterial strains for control pure BiVO$_4$ and BiVO$_4$/PVA

Bacterial strain (*E. coli*)	Inhibition zone diameter (mm)	MIC (µg mL^{-1})
Control	16	>90
BiVO$_4$	24	60–65
BiVO$_4$/PVA	28	20–25
Bacterial strain (*Staphylococcus aureus*)		
Control	16	>90
BiVO$_4$	26	45–50
BiVO$_4$/PVA	30	25–30

Table 3 Represents the inhibition zone diameter and calculated MIC value of bacterial strains for control pure BiVO$_4$ & BiVO$_4$/PVA

Fungal strain (*Rosselinia nacatrix*)	Inhibition zone diameter (mm)	MIC (µg mL^{-1})
Control	18	>85
BiVO$_4$	24	0.5–0.10
BiVO$_4$/PVA	29	0.05–0.09
Fungal Strain (fussarium spp)		
Control	18	>85
BiVO$_4$	28	25
BiVO$_4$/PVA	30	10

BiVO$_4$ nanocomposite is attributable to the production of reactive oxygen species, such as hydroxyl radicals, which may negatively impact bacterial cell membranes and disturb biological processes. The combined actions of the PVA polymer and BiVO$_4$ nanoparticles lead to the strong antibacterial action. The regulated expulsion of antimicrobial compounds from the PVA/BiVO$_4$ nanocomposite matrix may offer long-term antibacterial assurance, even after prolonged usage or ageing.[43] The simultaneous actions of the PVA polymer matrix and BiVO$_4$ nanoparticles lead to nanocomposites strong antibacterial properties. The amalgamation of the two elements produces a more effective antibacterial substance than either one alone. The introduction of BiVO$_4$ nanoparticles into the PVA matrix enhances the surface area of the nanocomposite, facilitating more interaction with bacterial cells and improving antibacterial characteristics. The same procedure holds for antifungal activity.[44] Disc diffusion experiments use fungal strains (*Rosselinia nacatrix* and fussarium spp) rather than bacteria to determine zones of fungal growth inhibition. Broth dilution tests to establish the minimal inhibitory doses against fungus.[45] Live/dead spotting and microscopy are used to visualize the impact on fungal cells (Fig. 15). The size of inhibition zone provides a quantitative measure of nanocomposite antifungal activity. Moreover, the antibacterial and antifungal experiments were

performed multiple times to evaluate possible errors in the evaluation. Fig. 16(a and b) highlights the antimicrobial and antifungal activity with errors bars, and it was observed that there were low percentage errors from the calculated data. For instance, the control group show the deviations of (0.25 and 0.6) for (*E. coli* and S aureus) and (0.25 and 0.8) for, while the BiVO$_4$/PVA show the deviation of (0.59 and 0.3) for *E. coli* and S aureus. The small error bar for control show that the antimicrobial and antifungal activity for control are very consistent. The error bar for pure BiVO$_4$ and BiVO$_4$/PVA show that antimicrobial effects of these varies between experimental repeats (Table 2). This could be due to measurement techniques and biological differences and material nature (Table 3).

6 Conclusion

Pure BiVO$_4$, Pure PVA and BiVO$_4$/PVA (1 : 1), BiVO$_4$/PVA (1 : 2), and BiVO$_4$/PVA (1 : 3) nanocomposites were synthesized by coprecipitation method to check the photocatalytic activity against reactive yellow dye. In comparison to pure BiVO$_4$ and PVA, the BiVO$_4$/PVA nanocomposite has superior photocatalytic, antibacterial, and antifungal characteristics. The BiVO$_4$/PVA nanocomposite features a red-shifted absorption

peak at 513 nm, which allows for visible light absorption. The EDX analysis reveals the purity of the sample. The band gap energy is reduced from 2.7 eV for PVA and 2.4 eV for BiVO$_4$ to 2.03 eV for BiVO$_4$/PVA (1:3), which improves visible light absorption. SEM image indicate three dimensional agglomoration of irregular shaped nanoparticles for BiVO4/PVA (1:3) with a crystallite size of 71 nm for pure BiVO$_4$. FTIR examination validates the presence of PVA-O, C–H, and O–H bonds in the nanocomposite. When exposed to UV-vis light, the BiVO$_4$/PVA (1:3) nanocomposite shows the maximum photocatalytic degradation of 91.3% for reactive yellow dye. According to scavenger experiments, the principal reactive species responsible for dye degradation are superoxide and hydroxyl radicals. Antifungal activity was proven against the fungus Rosselinia necatrix and Fusarium spp. BiVO$_4$ nanoparticles and the PVA polymer matrix work together synergistically to improve the efficiency of the BiVO$_4$/PVA nanocomposite. *Via* photogenerated reactive oxygen species, BiVO$_4$ offers potent oxidizing capability, while PVA improves the stability and dispersibility of the nanocomposite. Due to its distinct optical, structural, and functional characteristics, the nanocomposite is a good fit for antibacterial treatments, water purification, and various other pollution control methods.

Author contributions

Rabia Shahzad, Abdallah M. Elgorban, Hind A. AL-Shwaiman, Sabah Kausar, Aqsa Ashraf and Sumera Afsheen contributed to conceptualization, methodology, and original/initial draft, Tahir Iqbal contributed towards conceptualization, formal analysis, and Supervision. Sumera Afsheen Atif Mossad Ali, M. A. Sayed and Zain Ashfaq contributed resources, validation, editing, and review of the final draft.

Conflicts of interest

The authors declare that they have no competing interests.

Data availability

All data generated or analyzed during this study are included in this published article.

Acknowledgements

References

1 R. Roy, An Introduction to water quality analysis, *Essence Int. J. Env. Rehab. Conser.*, 2019, **9**(1), 94–100.

2 T. A. Aragaw, F. M. Bogale and B. A. Aragaw, Iron-based nanoparticles in wastewater treatment: a review on synthesis methods, applications, and removal mechanisms, *J. Saudi Chem. Soc.*, 2021, **25**(8), 101280.

3 S. Shukla, R. Khan and A. Daverey, Synthesis and characterization of magnetic nanoparticles, and their applications in wastewater treatment: a review, *Environ. Technol. Innov.*, 2021, **24**, 101924.

4 T. Krithiga, *et al.*, Persistent organic pollutants in water resources: fate, occurrence, characterization and risk analysis, *Sci. Total Environ.*, 2022, **831**, 154808.

5 P. Nidheesh, M. Zhou and M. A. Oturan, An overview on the removal of synthetic dyes from water by electrochemical advanced oxidation processes, *Chemosphere*, 2018, **197**, 210–227.

6 J. O. Eniola, *et al.*, A review on conventional and advanced hybrid technologies for pharmaceutical wastewater treatment, *J. Cleaner Prod.*, 2022, **356**, 131826.

7 M. Kifetew, *et al.*, Adsorptive removal of reactive yellow 145 dye from textile industry effluent using teff straw activated carbon: optimization using central composite design, *Water*, 2023, **15**(7), 1281.

8 S. N. Kamati, J. Yan and J. Fan, A review on progresses in reactive dye-containing wastewater treatment, *Water Pract. Technol.*, 2024, **19**(7), 2712–2733.

9 J. Dhote, S. Ingole and A. Chavhan, Review on wastewater treatment technologies, *Int. J. Eng. Res. Technol.*, 2012, **1**(5), 1–10.

10 D. Chen and A. K. Ray, Removal of toxic metal ions from wastewater by semiconductor photocatalysis, *Chem. Eng. Sci.*, 2001, **56**(4), 1561–1570.

11 J. Hong, *et al.*, Recent advances in wastewater treatment using semiconductor photocatalysts, *Curr. Opin. Green Sustainable Chem.*, 2022, **36**, 100644.

12 D. Zhu and Q. Zhou, Action and mechanism of semiconductor photocatalysis on degradation of organic pollutants in water treatment: a review, *Environ. Nanotechnol., Monit. Manage.*, 2019, **12**, 100255.

13 J. Sun, *et al.*, Bismuth vanadate hollow spheres: Bubble template synthesis and enhanced photocatalytic properties for photodegradation, *Appl. Catal., B*, 2013, **132**, 304–314.

14 D. T. T. Trinh, *et al.*, Synthesis, characterization and environmental applications of bismuth vanadate, *Res. Chem. Intermed.*, 2019, **45**, 5217–5259.

15 B.-R. Wulan, *et al.*, Non-noble-metal bismuth nanoparticle-decorated bismuth vanadate nanoarray photoanode for efficient water splitting, *Mater. Chem. Front.*, 2018, **2**(10), 1799–1804.

16 Q. Alijani, S. Iravani and R. S. Varma, Bismuth vanadate (BiVO$_4$) nanostructures: eco-friendly synthesis and their photocatalytic applications, *Catalysts*, 2022, **13**(1), 59.

17 S. Pramila, *et al.*, Green synthesis of bismuth vanadate nanostructures for efficient photocatalytic and biological studies, *Nano-Struct. Nano-Objects*, 2024, **39**, 101198.

18 O. M. Pardeshi, *et al.*, Sol gel auto-combustion synthesis of bismuth vanadate (BiVO$_4$) nanoparticles and its supercapacitor applications, *J. Mater. Sci.: Mater. Electron.*, 2023, **34**(26), 1817.

19 S. Lotfi, *et al.*, Recent progress on the synthesis, morphology and photocatalytic dye degradation of BiVO4 photocatalysts: A review, *Catal. Rev.*, 2024, **66**(1), 214–258.

20 R. R. Remya, *et al.*, Advancements in nanocomposites for wastewater treatment addressing emerging pollutants and contaminants, *Nanotechnol. Environ. Eng.*, 2024, **9**(1), 99–110.

21 Z. W. Abdullah, *et al.*, PVA, PVA blends, and their nanocomposites for biodegradable packaging application, *Polym.-Plast. Technol. Eng.*, 2017, **56**(12), 1307–1344.

22 T. S. Gaaz, *et al.*, Properties and applications of polyvinyl alcohol, halloysite nanotubes and their nanocomposites, *Molecules*, 2015, **20**(12), 22833–22847.

23 T. Sabu, *et al.*, *Polymer Composites, Macro-And Microcomposites,* Weinheim, Germany, John Wiley & Sons, 2012, vol. 1, pp. 356–358.

24 N. Ghazal, *et al.*, Surface and optoelectronic impacts of ZnO/BiVO4/MWCNT nanoheterostructure toward photodegradation of water contaminants, *Surf. Interfaces*, 2022, **33**, 102278.

25 M. Liaqat, *et al.*, Synthesis and characterization of ZnO/BiVO4 nanocomposites as heterogeneous photocatalysts for antimicrobial activities and waste water treatment, *Mater. Chem. Phys.*, 2024, **315**, 128923.

26 S. Selvarajan, *et al.*, Highly efficient BiVO4/WO3 nanocomposite towards superior photocatalytic performance, *Powder Technol.*, 2017, **307**, 203–212.

27 S. Chaiwichian, Synthesis of novel activated carbon/BiVO4 nanocomposite photocatalysts for degradation of organic compounds in wastewater, in *Journal of Physics: Conference Series*, IOP Publishing, 2022.

28 V. Sivakumar, *et al.*, BiVO4 nanoparticles: preparation, characterization and photocatalytic activity, *Cogent Chem.*, 2015, **1**(1), 1074647.

29 E. F. d. Reis, *et al.*, Synthesis and characterization of poly(vinyl alcohol) hydrogels and hybrids for rMPB70 protein adsorption, *Mater. Res.*, 2006, **9**, 185–191.

30 S. B. Aziz, *et al.*, Characteristics of poly(vinyl alcohol)(PVA) based composites integrated with green synthesized Al3+-metal complex: Structural, optical, and localized density of state analysis, *Polymers*, 2021, **13**(8), 1316.

31 P. Akhter, *et al.*, Montmorillonite-Supported BiVO4 nanocomposite: synthesis, interface characteristics and enhanced photocatalytic activity for dye-contaminated wastewater, *J. Ind. Eng. Chem.*, 2023, **123**, 238–247.

32 D. T. T. Trinh, *et al.*, New insight into the photocatalytic degradation of organic pollutant over BiVO4/SiO2/GO nanocomposite, *Sci. Rep.*, 2021, **11**(1), 4620.

33 E. J. Sisay, *et al.*, Visible-light-driven photocatalytic PVDF-TiO2/CNT/BiVO4 hybrid nanocomposite ultrafiltration membrane for dairy wastewater treatment, *Chemosphere*, 2022, **307**, 135589.

34 S. Kausar, *et al.*, Improving photocatalytic, antimicrobial properties, and enzymatic activity *via* ag doping in BiVO4 Photocatalysts using a simple co-precipitation technique and verified by theoretical analysis, *J. Inorg. Organomet. Polym. Mater.*, 2024, 1–17.

35 N. Wetchakun, *et al.*, Efficient photocatalytic degradation of methylene blue over BiVO4/TiO2 nanocomposites, *Ceram. Int.*, 2015, **41**(4), 5999–6004.

36 M. F. R. Samsudin, *et al.*, Photocatalytic degradation of real industrial poultry wastewater *via* platinum decorated BiVO4/g-C3N4 photocatalyst under solar light irradiation, *J. Photochem. Photobiol., A*, 2019, **378**, 46–56.

37 M. Liaqat, *et al.*, Comparative photocatalytic study of visible light driven BiVO4, Cu2O, and Cu2O/BiVO4 nanocomposite for degradation of antibiotic for wastewater treatment, *J. Chem. Phys.*, 2023, **159**(20), 204704.

38 M. Liaqat, *et al.*, Enhancing photocatalytic activity: investigating the synthesis and characterization of BiVO4/Cu2O/graphene ternary nanocomposites, *J. Photochem. Photobiol., A*, 2024, **446**, 115122.

39 C. Yu, *et al.*, Simultaneous hydrogen production from wastewater degradation by protonated porous g-C3N4/BiVO4 Z-scheme composite photocatalyst, *Sep. Purif. Technol.*, 2024, **335**, 126201.

40 H.-L. An, *et al.*, Sonocatalytic degradation of tetracycline by BiVO4/CuWO4 nanocomposites: operational parameters, sonocatalytic mechanism, and degradation pathways, *J. Mater. Sci.*, 2024, **59**(6), 2340–2360.

41 K. Drisya, *et al.*, Electronic and optical competence of TiO2/BiVO4 nanocomposites in the photocatalytic processes, *Sci. Rep.*, 2020, **10**(1), 13507.

42 A. Gomathi, *et al.*, Boosting the performance of solar light driven CeO2/BiVO4 anchored g-C3N4 nanocomposites: a systematic study toward the development of a photocatalytic and antibacterial activity, *Colloids Surf., A*, 2023, **673**, 131835.

43 A. Khan, *et al.*, In situ solid-state fabrication of Z-Scheme BiVO4/g-C3N4 heterojunction photocatalyst with highly efficient-light visible activity and their antibacterial properties against bacterial pathogens, *J. Mol. Struct.*, 2024, **1300**, 137222.

44 K. Sarvani, L. Hiremath and N. M. Prabu, Design and study of BiVO4/MnCo2O4 nanocomposites for visible light-driven antibacterial applications, *Curr. Sci.*, 2023, **124**(2), 183–189.

45 M. H. de Matos Rodrigues, *et al.*, Effect of pH on the synthesis of BiVO4 to improve photocatalysis and antimicrobial properties, *Mater. Chem. Phys.*, 2023, **296**, 127198.